Palladium Nanoparticles by Electrospinning from Poly(acrylonitrile-*co*-acrylic acid)−$PdCl_2$ Solutions. Relations between Preparation Conditions, Particle Size, and Catalytic Activity

Mustafa M. Demir, Mehmet A. Gulgun, and Yusuf Z. Menceloglu

Faculty of Engineering and Natural Sciences, Sabanci University, Orhanli 34956 Istanbul, Turkey

Burak Erman*

Department of Chemical and Biological Engineering, Koc University, Rumelifeneri yolu, Sariyer 80910, Istanbul, Turkey

Sergei S. Abramchuk, Elena E. Makhaeva, and Alexei R. Khokhlov

Physics Department, Moscow State University, Moscow 117234, Russia

Valentina G. Matveeva and Mikhail G. Sulman

Tver Technical University, Tver 170026, Russia

Received August 8, 2003; Revised Manuscript Received January 12, 2004

ABSTRACT: Catalytic palladium (Pd) nanoparticles on electrospun copolymers of acrylonitrile and acrylic acid (PAN-AA) mats were produced via reduction of $PdCl_2$ with hydrazine. Fiber mats were electrospun from homogeneous solutions of PAN-AA and $PdCl_2$ in dimethylformamide (DMF). Pd cations were reduced to Pd metals when fiber mats were treated in an aqueous hydrazine solution at room temperature. Pd atoms nucleate and form small crystallites whose sizes were estimated from the peak broadening of X-ray diffraction peaks. Two to four crystallites adhere together and form agglomerates. Agglomerate sizes and fiber diameters were determined by scanning and transmission electron microscopy. Spherical Pd nanoparticles were dispersed homogeneously on the electrospun nanofibers. The effects of copolymer composition and amount of $PdCl_2$ on particle size were investigated. Pd particle size mainly depends on the amount of acrylic acid functional groups and $PdCl_2$ concentration in the spinning solution. Increasing acrylic acid concentration on polymer chains leads to larger Pd nanoparticles. In addition, Pd particle size becomes larger with increasing $PdCl_2$ concentration in the spinning solution. Hence, it is possible to tune the number density and the size of metal nanoparticles. The catalytic activity of the Pd nanoparticles in electrospun mats was determined by selective hydrogenation of dehydrolinalool (3,7-dimethyloct-6-ene-1-yne-3-ol, DHL) in toluene at 90 °C. Electrospun fibers with Pd particles have 4.5 times higher catalytic activity than the current Pd/Al_2O_3 catalyst.

1. Introduction

Metal nanoparticles are gaining importance in fields of physics (quantum optics), chemistry (catalysts), and nanotechnology. Chemical and physical properties of nanoscale metal clusters are quite different from those of bulk metals. The major difficulty in working with nanoparticles is their undesirable agglomeration to form larger particles. To prevent formation of such agglomerates, surfactants,[1,2] ligand exchange materials,[3,4] and polymeric carriers[5] are used extensively. One new approach can be deposition nanoparticles directly on electrospun fibers from solutions. In this approach the major difficulty of particle agglomeration can be eliminated.

Electrospinning is a fiber fabrication technique that produces continuous polymer fibers with diameters from nanometers to micrometers.[6] In the process, a polymer solution or melt is placed into a container that has a millimeter diameter nozzle. An electrical field of several kilovolts is applied between the nozzle and the substrate that also serves as the ground. Under applied electrical force, the polymer is ejected from the nozzle. The diameter of the jet is reduced significantly as it is deposited from the nozzle on to the template. As a result, a porous film, namely fiber mat composed of nanoscale thin fibers, is obtained.[7] Such thin fibers provide very high surface area-to-volume ratios and are of interest for many applications in nanofiber textiles, composite reinforcement, sensors, biomaterials, and membrane technology. The present work combines two methods of electrospinning and reduction of metal salts in hydrazine solution that produces large surface area fibers with well-separated nanosized Pd particles.

Nanoclusters of palladium on PAN-AA nanofibers were synthesized by direct reduction of $PdCl_2$ in aqueous hydrazine media. A similar electrospinning technique was performed with reduced Ag particle in feed solution.[8] Previously, hydrothermal reduction,[9] aqueous solution of alkali borohydrides,[10] and hydrazine media[11] were used to reduce metallic salts to metal particles. Recently, Gui et al. reported on the reduction of first-row [3d] transition-metal complexes in aqueous hydrazine solution.[11]

A number of studies were performed to synthesize noble metal particles of different elements starting from micellization of polymeric templates in aqueous medium.[12,13] The important key factor of this method is to synthesize a soluble copolymer making micellar[13] or dendritic[12] structures which have enough space at the core for smaller metal salt molecules. Following the reduction process of the metal salt, uniform sized stable metal nanoparticles were formed. This is a result of fine control over micelle morphology. Various parameters

* Corresponding author: phone +90 (212) 338 17 04; Fax +90 (212) 338 15 48; e-mail berman@ku.edu.tr.

10.1021/ma035163x CCC: $27.50
Published on Web 02/13/2004

Table 1. Compositions of PAN-AA Copolymer Solutions

solution	AA, mol %	polymer concn (wt %)	$PdCl_2$ (wt %)[a]	Pd (wt %)[b]
A	5.4	8	0.63	0.4
B	5.4	8	1.25	0.75
C	8.1	8	1.25	0.75
D	5.4	8	8.3	5

[a] Weight of $PdCl_2$ divided by weight of polymer. [b] Weight of Pd atom divided by weight of polymer.

like type of reducing agent and pH of solution and type of copolymer (diblock, branched, or star)[14] affect the nanoparticle size as well. In the case of PAN-AA, the amount of AA controls the morphology of cluster size.

Transition-metal particles have found widespread application in catalysis, solar energy absorption, and magnetic materials. Palladium is known for its selective catalytic activity in hydrogenation of dienes and olefins,[5] enamine synthesis,[15] and amination of halopyridines.[16] Ledoux et al. observed that carbon nanotube supported Pd accelerates selective hydrogenation of cinnemaldehyde significantly.[17] Reneker and co-workers utilized electrospun fibers for catalytic purposes.[18] In the present work we also report on the catalytic activity of Pd nanoparticles on nanofibers for the hydrogenation reaction of unsaturated alcohols. The products of this reaction are intermediates in the synthesis of vitamins A, E, and K.

2. Experimental Section

The synthesis of PAN-AA copolymers was accomplished in dimethylformamide at 68 °C in the presence of water (2 wt %) and malic acid (0.015 wt %) in an argon atmosphere. A small amount of water was added to increase the molecular weight of the synthesized copolymers by radical polymerization reaction. Azobis(isobutyronitrile) (AIBN) was used as an initiator. Monomer concentration was 35%. The polymerization reaction was completed in 11 h.

The polymers used in the experiments have (viscosity molecular weight) M_η in the range of 100 ± 20 kg mol^{-1}. The molecular weights of the synthesized copolymers were characterized by viscosimetry. The intrinsic viscosity was measured in 0.2 M LiCl solution in DMF at 25 °C using an Ubbelohde viscosimeter with inner diameter 0.1 mm. Solution pH used for viscosimetry was in the range of 6.4−6.8. Two different compositions of copolymers were prepared: (i) 5.4% AA and (ii) 8.1% AA. A 500 MHz NMR (Varian) was employed to determine the AA content on the copolymer backbone by peak integration technique. It is found that composition of AA monomer in solution is approximately equal to the composition of AA on the backbone.

$PdCl_2$ and PAN-AA are dissolved in DMF at different concentrations as illustrated in Table 1. The solutions were prepared at room temperature by stirring to facilitate the dissolution of $PdCl_2$. Since the solutions are water sensitive, preparations were carefully carried out in dry environment.

The details of electrospinning process are explained elsewhere.[7] Four samples (*A, B, C, D*) were prepared from solutions (A, B, C, D). The concentration of the copolymers was kept constant at 8 wt % of the solution. An electrical field of 1.8 kV/cm was applied to all solutions, and the deposition time was adjusted to obtain a dense film. A matlike film was obtained on the grounded aluminum foil.

The electrospun fiber mat deposited on the cathode was removed easily and immersed into dilute hydrazine water solution. A dilute aqueous solution of hydrazine was prepared in the ratio of 1:200 ($V_{\text{hydrazine}}$:V_{water}). Aqueous hydrazine solution is a nonsolvent for both $PdCl_2$ and PAN-AA copolymer and a reducing agent for $PdCl_2$. Metallic Pd appears after several hours of reaction time in the immersed state. The color of the film turned dark gray, indicating that the Pd^{2+} ions are reduced to Pd^0 metal particles. The intensity of the color depends on the amount of $PdCl_2$ used. The electrospun mats were then washed with distilled water eight times and dried.

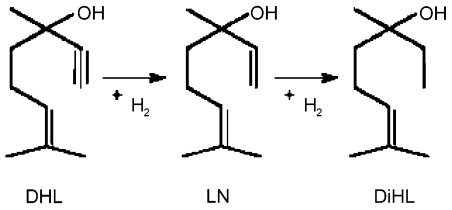

Figure 1. Hydrogenation reaction of dehydrolinalool (3,7-dimethyloktaen-6-in-1-ol-3) (DHL).

Characterization of Fibers and Metal Nanoparticles. Overall morphology of the fiber mats, fiber diameters, and the distribution and size of the palladium particles/agglomerates were investigated using conventional (JSM 840-A, JEOL, Tokyo, Japan) and low-voltage high-resolution FEG-SEMs (field emission gun scanning electron microscopes, ESEM-FEG, FEI, Eindhoven, Holland). Samples were either spun onto aluminum foils for SEM investigations or on copper grids for investigations with a transmission electron microscope (TEM) (JEM 2000FX, JEOL, Tokyo, Japan). The SEM resolution was adequate to determine the diameter of the fibers and the size of the palladium agglomerates. The primary particle and crystallite sizes of the Pd particles were determined using a TEM. The small subunits are defined as the primary particles. The particle may consist of several subunits. Energy dispersive spectroscopy (EDS) attached to the TEM was employed to determine the chemical composition of the polymer fibers as well as the chemistry of the particles on them. For TEM and high-voltage SEM investigations, samples were coated with carbon. Several samples were studied with the low-voltage SEM (at 0.8−2 kV) without coating to determine whether the Pd particles are on or in the polymer fibers. X-ray analyses were performed using a powder diffractometer (Bruker AXS, D8 Advance, AXS, Karlsruhe, Germany). A piece of mat was placed on to the sample holder and was scanned over more than 20 times to improve the signal-to-noise ratio of the data. Scans were made from 30° to 90° (2Θ) with the speed of 0.02°/s. The size of the Pd particles was estimated from X-ray peak broadening in the diffractograms and from the TEM and SEM images. Fiber diameters were determined from TEM and SEM micrographs. Average fiber diameter (AFD) and size of Pd particles were measured for all samples by using at least 40 representative data points.

Method of Hydrogenation at Static Conditions. Catalytic properties of PAN-AA copolymer containing Pd were investigated via hydrogenation of dehydrolinalool (3,7-dimethyloktaen-6-in-1-ol-3) (DHL). The procedure for determining catalytic activity measurements were described previously.[19,20] Catalytic activity and selectivity were reported as the amounts and types of reaction products. Figure 1 shows the hydrogenation reaction of acetylene alcohol (DHL). A selective hydrogenation of dehydrolinalool leads to the formation of linalool (3,7-dimethyl-1,6-octadien-3-ol) (LH). In contrast, a nonselective process yields 3,7-dimethylokten-6-ol-3 (DiLH). Catalytic activity was estimated by the reaction rate W (m^3 H_2 s^{-1}/mol of Pd·mol of DHL), which was calculated as the ratio of hydrogen volume absorbed per unit time per mole of Pd and mole of DHL.

The copolymer solution (15×10^{-6} m^3) was introduced in a thermostatic reactor vessel. Toluene was used as a solvent. The total volume of the liquid phase is 32×10^{-6} m^3. The reactor was flushed by hydrogen three times, and then it was hermetically sealed. Hydrogen saturation was reached after 60 min with continuous agitation. Then the solution of DHL was added into the reactor vessel. The hydrogenation process was continued at constant agitation level of 960 shakes/min. During the reaction the amount of absorbed hydrogen was analyzed. For each sample, 5−9 tests were performed for different time periods.

Copolymers of PAN-AA with 5.4 and 8.1 mol % AA containing 0.75% Pd were analyzed (samples B and C). Before the

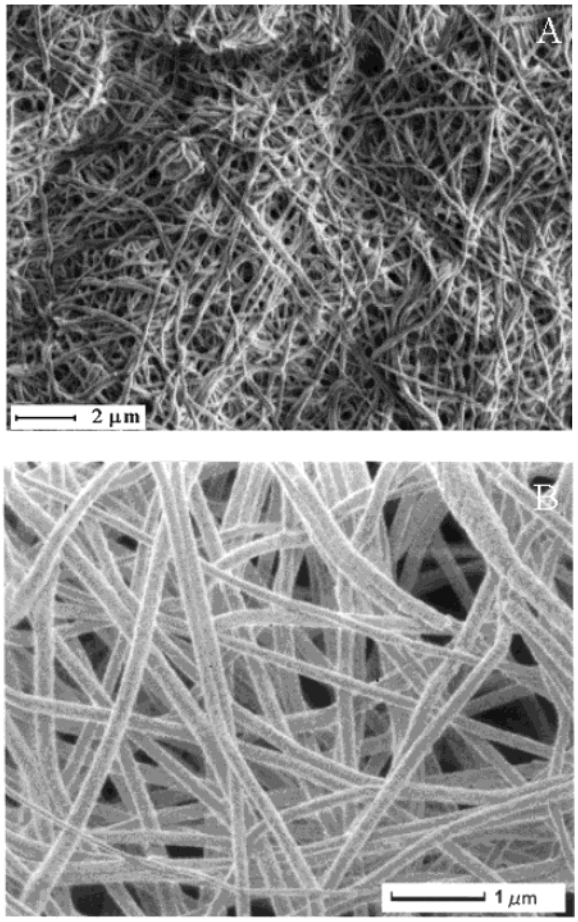

Figure 2. Electron microspcope images of nanofibers electrospun from 8 wt % PAN with (a) 5.4% mol AA and (b) 8.1% mol AA under 1.8 kV/cm.

measurements copolymer samples were dried at 40° C for 6−8 h. The mole number of $PdCl_2$ is equal to that of Pd after reduction. The molecular weight of $PdCl_2$ is 177 g/mol, whereas that of Pd is 106 g/mol; therefore, the weight fraction of the Pd to polymer is (106/177) times lower than that of $PdCl_2$.

3. Results

PAN-based fibers, precursor of carbon fibers, having diameters 165 ± 35 nm were obtained by applying an electrical field of 1.8 kV/cm to the polymer solutions. Precise measurements of fiber diameters were performed on 20 test fibers. PAN was chosen with its comonomer AA as a model system. Copolymers with (a) 5.4 mol % and (b) 8.1 mol % AA were successfully electrospun from DMF. Figure 2 shows representative electron microscope images of PAN-AA nanofibers, electrospun from these two copolymer solutions, (a) 5.4 mol % and (b) 8.1 mol %. Electrospun mats were easily detached from the grounded Al foil with a size of 3 × 5 cm^2, and their specific surface area was estimated from their diameter to be on the order of 25 m^2 per gram polymer.

Characterization of Pd Nanoparticles. Characterization of Pd particles was performed mainly on four samples which are obtained from electrospinning of solution A, B, C, and D. Pd particles were produced inside the electrospun mats by reducing $PdCl_2$ with hydrazine hydrate. Pd particles were detected by XRD, imaged by electron microscopy, and identified by EDS. Particle agglomerations were determined by X-ray peak broadening, high-resolution SEM, and TEM techniques.

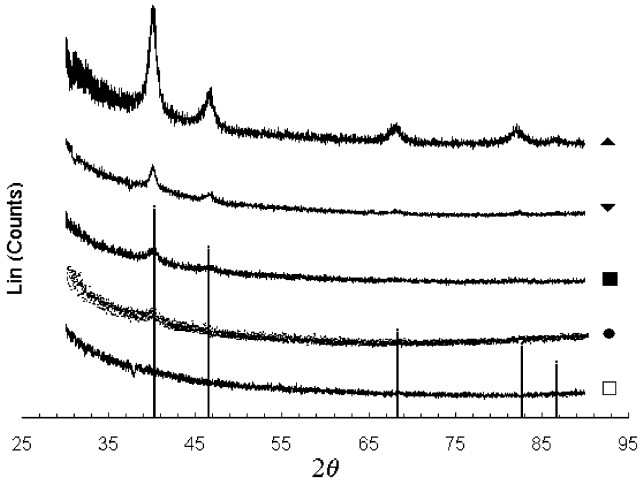

Figure 3. X-ray diffracion peaks of mat PAN with (□) 5.4 mol % AA and 1.25% $PdCl_2$ before the reduction process, (●) 5.4 mol % AA and 0.63% $PdCl_2$ after the reduction process, (■) 5.4 mol % AA and 1.25% $PdCl_2$ after the reduction process, (▼) 8.1 mol % AA and 1.25% $PdCl_2$ after the reduction process, and (▲) 5.4 mol % AA and 8.3% $PdCl_2$ after the reduction process.

Aqueous hydrazine in a basic solution is a powerful reducing agent, i.e., an electron donor.[21] The redox reaction of $PdCl_2$ in hydrazine solution is illustrated as follows:

$$N_2H_4(l) + 2PdCl_2 \rightarrow N_2(g)\uparrow + 2Pd^0(s)\ \text{[grayish black]} + 4HCl \quad (1)$$

The oxidation−reduction reaction proceeds with the appearances of bubbles on the electrospun fibers. These bubbles are the N_2 gas according to eq 1.

Figure 3 illustrates the X-ray diffraction pattern for PAN-AA with different amounts of comonomer and $PdCl_2$ before and after the reduction process of Pd cation. Five peaks were detected on the X-ray diffraction pattern between 30° and 90°. The main peak appeared around $2\Theta = 40.1°$ corresponding to the (111) peak of Pd. The other four peaks were at 46.6°, 68.1°, 82.1°, and 86.6°. The bars in the graph are from the JCPDS (Joint Committee on Powder Diffraction Standards) reference diffraction data file for Pd. The diffraction peaks from the fiber mats with Pd matches the reference for synthetic Pd. The curve labeled with the open square shows the XRD spectrum of the electrospun mat before the reduction process. The difference between this curve and other X-ray diffractions shown in the Figure 3 indicates reduction process from Pd cation to Pd metal in aqueous hydrazine solution. The full width at half-maximum (fwhm) of the spectra indicates different particle sizes. The dimensions of the Pd particles were estimated by using Debye−Scherer formula ($\beta = 0.9\lambda/(\text{fwhm} \cos\theta)$).[22] β is the size of the Pd crystals, presented in the fifth column of Table 2. The fwhm values of the diffraction peaks are given in the fourth column of Table 2. The calculated average size of Pd particles was 11.5 nm when acrylic acid content of copolymer is 5.4% mol and 14.5 nm when acrylic acid content is 8.1% mol. The sixth column of Table 2 corresponds to the approximate number of crystallites in average agglomerate whose size is determined by electron microscopy. Möller and Spatz[23] pointed out that using micellar diblock copolymer template which is poly(styrene-*b*-2-vinylpyridine), a regular arrangement of 6 nm gold particles with an

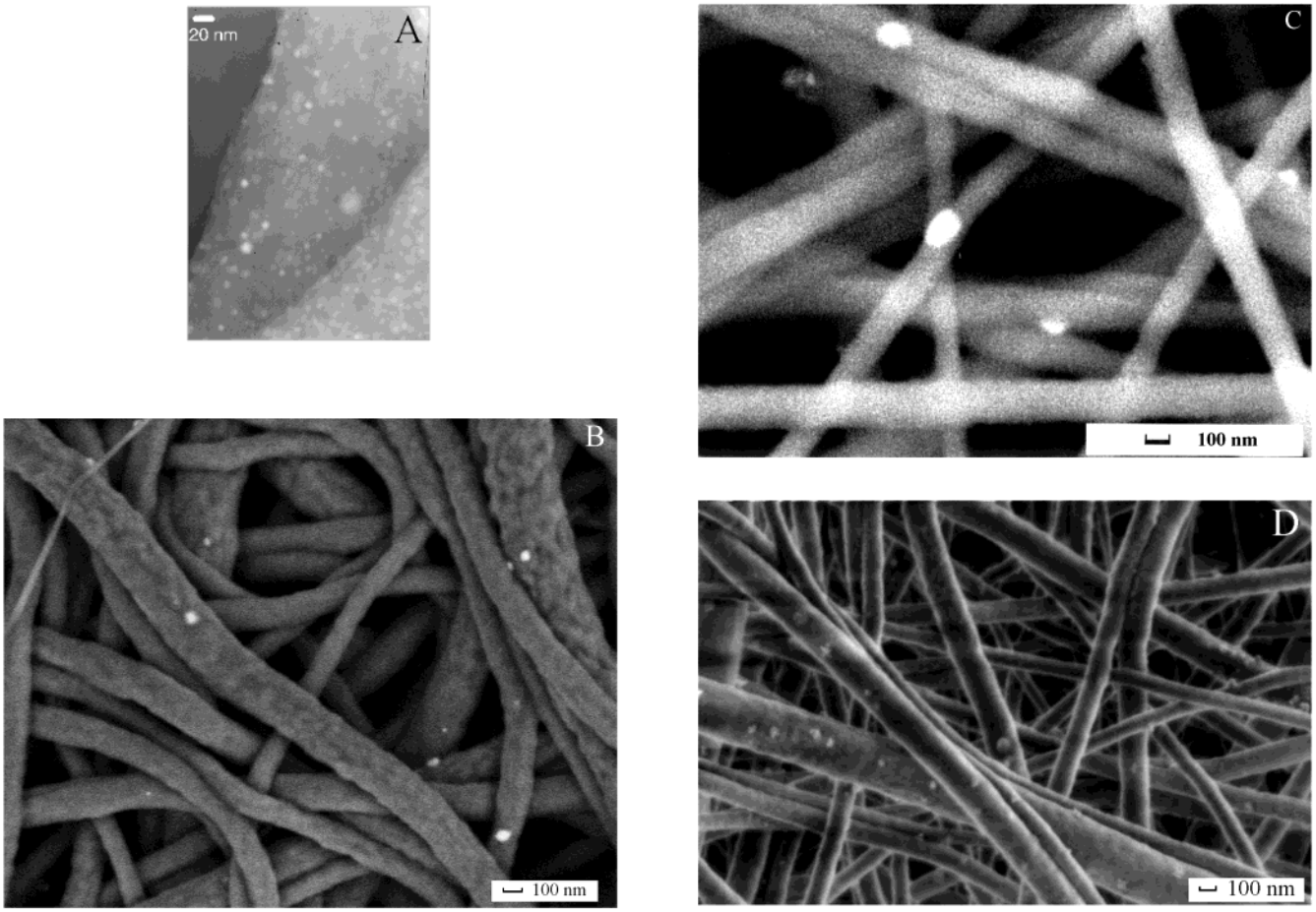

Figure 4. Electron microspcope images of PAN-AA fibers with generated Pd nanoparticles: (a) sample *A*, (b) sample *B*, (c) sample *C*, and (d) sample *D*. Sample A is magnified 300K times and the others 50K times.

Table 2. Dimensions of Electrospun PAN-AA Fibers and Pd Particles

sample	peak of AFD distributions (nm)[a]	peak of Pd particle diam distributions (nm)[a]	fwhm (deg)	Pd crystallite diam calcd (nm)[b]	av no. of crystallites in particles (agglomerates)[c]
A	100	10	0.741	14.1	0.72
B	180	20	0.904	11.5	1.74
C	150	60	0.721	14.5	4.14
D	165	30	0.973	10.7	2.8

[a] Measured and calculated from TEM images. [b] Calculated from X-ray peak broadening. [c] Column 3 is divided into column 5.

30 nm interparticle distance can be obtained. Toluene dissolves preferentially polystyrene block while polyvinylpyridine is almost insoluble. The solubility difference drives the formation of micelles. Forster and Keane[24] further found out that stable gold nanoparticles prepared by reduction of $HAuCl_4$ in polyvinylpyridine and metallopolymer composite. Particle size can be precisely tuned by the amount of metallopolymer mixed into the polymer matrix.

Electron Microscopy. Figure 4 shows the electron micrograph of mats with Pd nanoparticles in bright contrast. The particles appear to be spherical at this magnification. The atomic number difference between Pd and carbon facilitates imaging of the metal particles.

In Table 2, dimensions of PAN-AA fibers and Pd particles are presented. Four samples were electrospun from solutions of equal polymer concentration including two different constituents. Solutions A, B, and D contain the same copolymer, which has 5.4% AA, but $PdCl_2$ concentrations were different. Solutions B and C have equal amounts of $PdCl_2$; in contrast to solutions A and D, they include polymers with different AA contents.

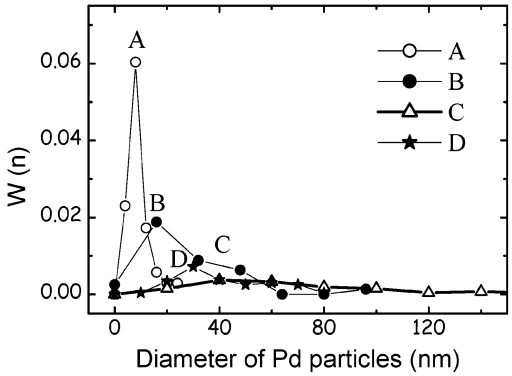

Figure 5. Distribution of palladium particle size for samples *A*, *B*, *C*, and *D*.

Results of measurements on fiber diameters are presented in the second column of Table 2. Peak values of the size distributions of Pd particles are presented in column 3 of Table 2. Figure 5 illustrates the normalized size distribution of the Pd particles inside electrospun mats for different samples. Precise measurements of

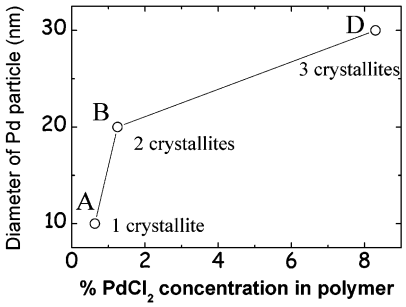

Figure 6. Pd particle size as a function of $PdCl_2$ concentration inside spinning solution.

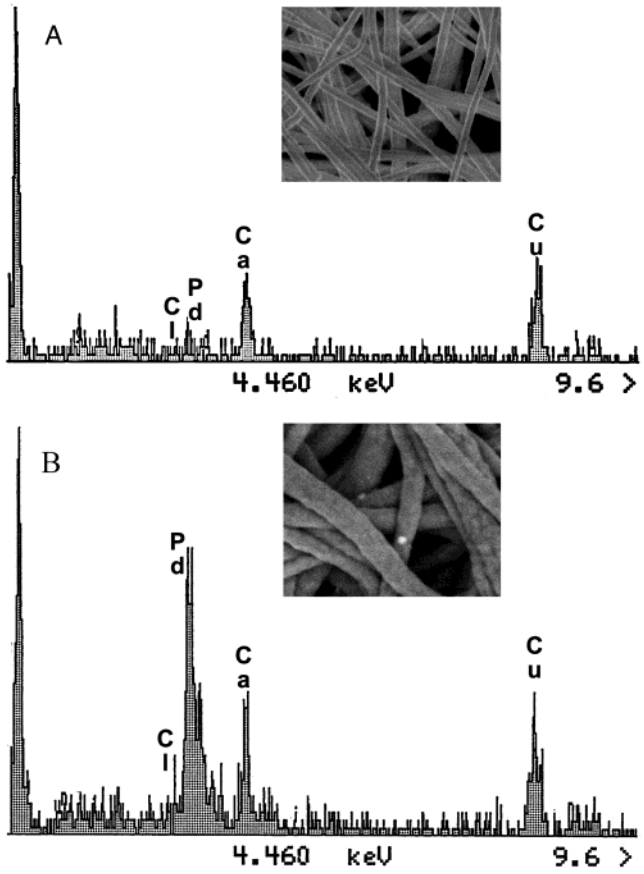

Figure 7. EDS of electrospun mats on showing the presence of Pd. The analyses were performed on regions where there was (a) no particle and (b) particle.

particle diameter were performed on 20 test particles. The particle size is larger when the AA amount is higher on polymer chains at constant $PdCl_2$ concentration in the spinning solution. Increasing the salt concentration ($PdCl_2$) led also to larger particles, but the effect was not as dominant as that of AA. Figure 6 shows the particle size observed on electron microscope as a function of $PdCl_2$ concentration inside the spinning solution, keeping the AA content constant on the polymer chain. Particle size increases as the $PdCl_2$ concentration increases. It appears that Pd particle size depends on the amount of comonomer AA and $PdCl_2$ concentration in the initial solution.

EDS. EDS attached to the TEM was employed to identify Pd metal particles. Figure 7a,b illustrates the energy-dispersive spectra collected from two regions which are shown at inset on electrospun mats: (a) region without and (b) region with Pd particles. The fiber mats were obtained from electrospinning of 8 wt % of PAN copolymers with 5.4% AA solution and 1.25 wt % $PdCl_2$ after the reduction process of Pd cation (sample *B*). Along with the presence of Pd peak, Ca and Cu peaks are also seen in the spectrum. The source of Ca may be the tap water used for precipitation of the polymer after finishing the polymerization reaction. The copper peak comes from the TEM grid. $PdCl_2$ is homogeneously distributed inside the fibers. The absence of the Cl peak on the spectra indicates that Pd cations are almost completely reduced. Hydrazine molecules penetrate inside the nanofibers and reduce the Pd cations. Pd atoms move to the perimeter of the fibers and agglomerate. High-resolution electron microscope images demostrate that the particles are on the surface of the nanofiber. Cl anions of the salt are removed during washing. EDS analysis was performed on Pd reduced samples and Cl ions were not detected.

Table 3. Catalytic Properties of Electrospun Fibers of Copolymers of PAN-AA Containing $PdCl_2$ and Pd Nanoparticles[a]

		selectivity *S*, %		
catalyst	reaction rate *W*, m^3 H_2/mol Pd·mol DHL	DHL	LN	DiHL
Copolymer (PAN-AA) + $PdCl_2$ (Before the Reduction)				
A	4.7		98.7	1.3
B	4.3	0.2	99.2	0.6
C	1.2		99.8	0.2
Copolymer (PAN-AA) + Pd (After the Reduction)				
A	11.3		100	
D	0.3	0.4	95.8	3.8
Pd/Al_2O_3 (0.5%)	2.5	0.5	95.6	3.9

[a] Experimental conditions: temperature = 90 °C; solvent = toluene; intensity of shaking = 960 sh/min; ratio = DHL mol/Pd mol = $1/7.7 \times 10^{-4}$.

Catalytic Activity of Pd on Electrospun Fibers. The catalytic activity of PAN-AA fibers, containing 5.4% and 8.1% of AA and variable content of Pd, was studied. The effect of the fraction of AA units, Pd concentration, and Pd state ($PdCl_2$ or metallic Pd after reduction by hydrazine) on the catalytic activity was analyzed. Results of the investigation of catalytic properties of Pd on electrospun fibers are presented in Table 3. It should be noted that, in all cases, the increase of AA fraction in copolymer from 5.4% to 8.1% leads to a decrease of reaction rate. This fact can be explained by the larger sizes of Pd nanoparticles in the case of copolymer containing 8.1% AA units which results in the decrease of catalytically active Pd surface. An increase of Pd content in fibers leads to the decrease of reaction rate and catalytic activity. The analysis of catalytic activity of electrospun fibers containing Pd reduced by hydrazine hydrate shows that catalytic activity increases twice in comparison with the reduction by hydrogen; also, selectivity achieves its maximum value (compare the two *A* rows of Table 3). The catalyst PAN-AA (5.4% AA) containing 0.4% of reduced Pd (without additional modification) is the most active and selective. The samples were characterized not only by high catalytic properties but also by stability and suitability for industrial processing. When compared to the current catalyst, i.e., Pd particles on Al_2O_3 supports, the catalytic activity of the Pd nanoparticles in electrospun fibers was found to be 4.5 times higher than that of Pd/Al_2O_3 (compare rows 7 and 9 in Table 3). This difference results from differences in the chemical structure of the supporting materials. Organic supports, like polymeric

fibers, work better than inorganic supports in organic reactions.

4. Discussion

Control of particle size and its dispersion is one of the main goals of nanocomposite preparation technology. There are two different levels of particle sizes in our experiments. Comparison of columns 3 and 5 of Table 2 shows that the size of Pd crystallites estimated from X-ray diffraction data differs from the data obtained for Pd particle sizes from electron microscopy images. Several primary particles (single crystallites) whose sizes were determined by X-ray agglomerate together to form a cluster that is imaged in SEM. The small subunits are defined as primary particles. They are single grains (crystallites) that form the clusters. Several high-resolution images indicated that the Pd particles were clusters of smaller crystallites. It is possible to estimate the average number of primary particles (crystallites) in such clusters. Two or four primary particles constitute each cluster when the AA concentrations are 5.4% and 8.1%, respectively (samples *B* and *C*). In the case of sample *A*, the size of the particles observed with an electron microscope is equal to or smaller than the crystallite size detected by X-ray diffractograms. Small crystals imaged by the electron microscope may not be detected by XRD due to the small crystal effect alone.[22] Most of the Pd particles are single crystallites when the $PdCl_2$ concentration in the initial solution is 0.6 wt % and the AA content is 5.4 mol %. When $PdCl_2$ concentration was increased six times on the same polymer (sample *D*), three crystallites form an agglomerate on the average.

The amount of acrylic acid on the polymer backbone is the dominant parameter affecting the size of the primary Pd particles. As the comonomer amount increases, the shape of the main peak on the X-ray spectra becomes narrower and the crystallite size becomes larger. A possible explanation of this observation is as follows: The comonomer, acrylic acid, serves as a host for the Pd cation. The Pd cation is attracted to acrylic acid group due to an electrostatic interaction. During the reduction process, Pd ion becomes neutral (Pd atom) which can dissociate easily from the acid groups. The Pd atoms come together and nucleate as primary Pd particles whose size can be estimated from the X-ray spectra. Since nucleation of metal particles takes place around acrylic acid groups, the amount and dispersion of acrylic acid on the polymer chain can directly determine the size and dispersion of the palladium crystallites formed. Electrostatic interaction of carboxyl anions and Pd cations cannot be considered as a driving force determining the particle size. When electrostatic attraction disappears, secondary forces become dominant and particles adsorb on the fibers. The radii of the Pd particles are several times the contour length of the macromolecule. The molecular weight of the copolymer is on the order of 100 kg.[12]

Increasing salt concentration increases the number of nucleation sites, namely particle density on the fibers. Consequently, particle size and dispersion can be tuned by the amount of $PdCl_2$ and composition of the copolymer (i.e., AN to AA ratio). For catalyst applications, the size of the Pd particles produced plays an important role. Smaller particles have larger surface area and accelerate the reaction rate. The area of Pd particles inside per gram of polymer is estimated approximately as 0.1 m^2 (sample *B*). The amount of Pd on the electrospun fiber mat is on the order of 50 mg/g. The present experimental technique does not allow for the determination of the amount of particles lost during rigorous washing of Pd from the surface.

Acknowledgment. This work was sponsored by NATO SfP-973925. The authors thank Mr. Atilla Alkan from Brissa for his helpful electron microscope works.

References and Notes

(1) Yonezawa, T.; Imamura, K.; Kimizuka, N. *Langmuir* **2001**, *17*, 4701−4703.
(2) Bönnemann, H.; Brijoux, W.; Brinkmann, R. *J. Mol. Catal.* **1994**, *86*, 129−134.
(3) Horswell, S.; Schiffrin, D. J. *J. Am. Chem. Soc.* **1999**, *121*, 5573−5578.
(4) Itoh, H.; Naka, K.; Chujo, Y. *Polym. Bull. (Berlin)* **2001**, *46*, 357−362.
(5) Hirai, H.; Yakaru, N. I.; Seta, Y.; Hodosima, S. *React. Funct. Polym.* **1998**, *37*, 121−131.
(6) Doshi, J.; Reneker, D. H. *J. Electrostat.* **1995**, *35*, 151−159.
(7) Demir, M. M.; Yilgor, E.; Yilgor, I.; Erman, B. *Polymer* **2002**, *43*, 3303−3309.
(8) Yang, Q. B.; Li, D. M.; Hong, Y. L.; Li, Z. Y.; Wang, C.; Qui, S. L.; Wei, Y. *Synth. Met.* **2003**, *137*, 973−974.
(9) Li, Y. D.; Li, L. Q.; Liano, H. W.; Wang, H. R. *J. Mater. Chem.* **1999**, *9*, 2675−2679.
(10) Wonterghem, J. van; Morup, S.; Koch, C. J.; Wells, S. *Nature (London)* **1986**, *322*, 622−625.
(11) Gui, Z.; Fan, R.; Mo, W.; Chen, X.; Yan, L.; Hu, Yuan. *Mater. Res. Bull.* **2003**, *38*, 169−176.
(12) Bronstein, L. M.; Sidorov, S. N.; Gourkova, A. Y.; Valetsky, P. M.; Hartmann, J.; Bruelmann, M.; Cölfen, H.; Antonietti, M. *Inorg. Chim. Acta* **1998**, *280*, 348−354.
(13) Sidorov, S. N.; Bronstein, L. M.; Valetsky, P. M.; Hartmann, J.; Cölfen, H.; Schnablegger, H.; Antonietti, M. *J. Colloid Interface Sci.* **1999** *212*, 197−211.
(14) Hedden, R. C.; Bauer, B. J.; Smith, A. P.; Gröhn, F.; Amis, E. *Polymer* **2002**, *43*, 5473−5481.
(15) Willis, M.; Brace, G. *Tetrahedron Lett.* **2002**, *43*, 9085−9088.
(16) Basu, B.; Jha, S.; Midra, N. K.; Bhuiyan, M. H. *Tetrahedron Lett.* **2002**, *43*, 7967−7969.
(17) Ledaux, M.; Vieira, R.; Pham-Huu, C.; Keller, N. *J. Catal.*, in press.
(18) Jia, H.; Zhu, G.; Vugrinovich, B.; Kataphinan, W.; Reneker, D. H.; Wang, P. *Biotechnol. Prog.* **2002**, *18*, 1027−1032.
(19) Sulman, E.; Bodrova, Y.; Matveeva, V.; et al. *J. Appl. Catal.* **1999**, *176*, 75−81.
(20) Bronstein, L.; Chernyshov, D.; Volkov, I.; Ezernitskaya, M.; Valetsky, P.; Matveeva, V.; Sulman, E. *J. Catal.* **2000**, *196*, 302−314.
(21) Cotton, F. A.; Wilkonson, G.; Gaus, P. L. *Basic Inorganic Chemistry*, 3rd ed.; John Wiley & Sons: New York, 1995; p 404.
(22) Cullity, B. D *Elements of X-ray Diffraction*, 2nd ed.; Addison-Wesley: Reading, MA, 1978; p 284.
(23) Spatz, J. P.; Roescher, A.; Möller, M. *Adv. Mater.* **1996**, *8*, 337−341.
(24) Forster, J. F.; Keane, L. *J. Electroanal. Chem.* **2003**, *554*−*555*, 345−354.

MA035163X